arXiv:1401.3278v2 [hep-ph] 25 Sep 2014

TUM-HEP-926-14

More Viable Parameter Space for Leptogenesis

Björn Garbrecht

Physik Department T70, James-Franck-Straße,
Technische Universität München, 85748 Garching, Germany

Abstract

Lepton flavour asymmetries generated at the onset of the oscillations of sterile neutrinos with masses above the electroweak scale can be large enough to partly survive washout and to explain the baryon asymmetry of the Universe. This opens up new regions of parameter space, where Leptogenesis is viable within the type-I seesaw framework. In particular, we find it possible that the sterile neutrino masses are substantially below 10^9 GeV, while not being degenerate. However, the required reheat temperature that is determined by the begin of the oscillations lies some orders of magnitude above the sterile neutrino mass-scale.

1 Introduction

While the type-I seesaw mechanism is a very plausible way of generating neutrino masses [1], it may turn out to evade experimental test. Augmenting the Standard Model (SM) by Majorana masses for the active neutrinos introduces nine new parameters (three masses, and in the PMNS matrix, three mixing angles, one Dirac and two Majorana phases), but there are nine extra numbers describing the masses and the couplings of the sterile neutrinos. Quite generically, the sterile neutrinos decouple from the SM either due to their high masses or their tiny couplings, such that these extra parameters remain practically unobservable.

Therefore, Leptogenesis [2] models based on the seesaw mechanism may likewise escape from direct tests. Nonetheless, the requirement of successful Leptogenesis is very useful in order to gain more constraints on the parameter space of the seesaw model, in particular when embedded in more general beyond the SM (BSM) frameworks. A very well known example is the lower bound on the masses of the sterile neutrinos, $2 \times 10^9\,\mathrm{GeV}$ [4, 3], which consequently implies a lower bound of $3 \times 10^9\,\mathrm{GeV}$ on the reheat temperature of the Universe (assuming a vanishing initial abundance of the sterile neutrinos).

Numerous loopholes to this bound arise when considering extensions of the SM beyond the seesaw scenario (we refer here always to the type-I variant), see *e.g.* Ref. [5].

Notable are therefore the few possibilities that allow for smaller sterile neutrino masses and lower reheat temperatures, but that yet rely on the minimal seesaw mechanism, thus avoiding a further proliferation of free parameters. The most well-known of these is resonant Leptogenesis, relying on the enhancement of the lepton-number violating charge-parity (CP) asymmetry due to the mixing of nearly mass-degenerate sterile neutrinos [6, 7, 8, 9, 10, 11, 12]. Besides aiming for small sterile neutrino masses, it should also be of general interest to fully chart the viable parameter space for Leptogenesis based on the minimal seesaw mechanism.

Here, we consider Leptogenesis from a source term that conserves lepton number but violates the individual flavours. Its presence was first pointed out in Ref. [13], and it was subsequently studied in a more accurate manner in Refs. [14, 15, 16]. We refer to it as the ARS scenario after the names of the authors of Ref. [13]. It is based on the usual seesaw model given by the Lagrangian

$$\begin{aligned}\mathcal{L} =& \frac{1}{2}\bar{N}(\mathrm{i}\partial\!\!\!/ - M)N + \bar{\ell}\mathrm{i}\partial\!\!\!/\ell + \bar{\mathrm{R}}\mathrm{i}\partial\!\!\!/\mathrm{R} + \partial^\mu\phi^\dagger\partial_\mu\phi \\ & -\bar{\ell}Y^\dagger N\tilde{\phi} - \bar{N}Y\ell\tilde{\phi}^\dagger - \phi^\dagger\bar{\mathrm{R}}h\ell - \phi\bar{\ell}h^\dagger\mathrm{R}\,,\end{aligned} \tag{1}$$

where ϕ is the Higgs doublet, $\tilde{\phi} = (\epsilon\phi)^\dagger$ and ϵ is the $\mathrm{SU(2)_L}$-invariant antisymmetric tensor. The sterile neutrinos are given by the Majorana spinors N_i, for which we assume three flavours, $i = 1, 2, 3$, and the left- and right-handed leptons of the SM by ℓ_a and R_a, where $a = e, \mu, \tau \equiv 1, 2, 3$. We choose the usual flavour bases for the sterile neutrinos where their mass matrix is $M = \mathrm{diag}(M_1, M_2, M_3)$ and for the SM leptons such that $h = \mathrm{diag}(h_e, h_\mu, h_\tau)$. For definiteness, we take $M_1 < M_2 < M_3$.

In the ARS scenario, oscillations of the sterile neutrinos are the dominant source of flavour asymmetries (that conserve total lepton number) in the SM leptons ℓ at temperatures $T \gg M_i$. The sterile neutrino masses are typically taken to be at the GeV scale or below [13, 14, 15], such that the couplings Y are suppressed enough (note the seesaw relation $m_\nu = Y^t M^{-1} Y v^2/2$, with m_ν the mass matrix of the SM neutrinos and $v = 246\,\mathrm{GeV}$) that the flavoured asymmetries are only weakly washed out prior to the electroweak phase transition (EWPT) at the temperature $T_{\mathrm{EW}} \approx 140\,\mathrm{GeV}$, where baryon-number ($B$) violating sphaleron processes freeze out. In Ref. [15], it is demonstrated that in spite of the low mass scale of the sterile neutrinos, no degeneracy is necessary in order to account for the observed baryon asymmetry of the Universe (BAU).

We add here for clarity that in the present paper, we use the term washout in both situations, when lepton-number violation (LNV) can be neglected for $M_i \ll T$ and when helicity flips through the Majorana masses effectively violate lepton number once the temperature is of order M_i. We refer to the former case, that yet affects the flavoured asymmetries as flavoured washout and the latter case as LNV washout. The case $M_i \ll T$ is relevant for the original ARS scenario, where lepton number remains effectively conserved at times before sphalerons freeze out. Indeed, since the sterile neutrinos are approximately chiral, one may attribute in that situation lepton number to these particles. Transitions through the sterile neutrinos can however lead toward chemical equilibrium between the different flavours ℓ_a. If chemical equilibrium is fully established, there

remain no individual asymmetries, due to complete flavoured washout. It is essential though, that the transitions to sterile neutrinos partly take place and affect the individual flavours in a quantitatively different manner. The individual flavoured asymmetries are then partly hidden from weak sphaleron transitions within the sterile neutrinos, what can result in a net baryon asymmetry.

Here, we propose that ARS-type Leptogenesis is also viable with sterile neutrinos above the electroweak scale, more precisely in the mass range from $10^3\,\mathrm{GeV}$–$10^{11}\,\mathrm{GeV}$ and mass ratios of order one. For the subsequent considerations, it is useful to recall the equilibrium neutrino mass [3] $m_\star = Y_\star^2 v^2/(2M_i)$, where $\Gamma_\star = Y_\star^2 M_i/(8\pi)$ and $H|_{T=M_i} = \Gamma_\star$ (H being the Hubble rate), such that $m_\star \approx 1.1 \times 10^{-12}\,\mathrm{GeV}$. In the present scenario, the flavour asymmetries are produced at temperatures above the masses M_i for all three N_i. Given that the observed neutrino mass-differences are larger than $m_\star$ and the large mixing angles, the asymmetries within each of the $\ell_{e,\mu,\tau}$ experience prior to the EWPT strong LNV washout, defined through the condition $\sum_i Y_{ai}^\dagger Y_{ia} M_i/(8\pi) \geq H$ (*i.e.* the washout rate for ℓ_a exceeds the Hubble rate) at some instance during the expansion of the Universe. Therefore, the conversion of the flavour asymmetries into a baryon asymmetry is less efficient than in the usual ARS scenario. However, the mass differences of the SM neutrinos are not too far above $m_\star$, such that there should be parametric regions where the washout of the asymmetries is not prohibitively strong. To demonstrate quantitatively that this is indeed a viable option, we properly include in this work both the effects from flavoured washout and LNV washout, that take place after the creation of the flavoured asymmetries from oscillations but before the sphaleron freeze-out around the EWPT. It turns out that the stronger washout compared to the usual ARS scenario can be made up for by larger initial asymmetries.

We mention now some similarities and differences with related papers. In Ref. [17], the see-saw model is constrained by certain flavour symmetries. As a result, N_1 couples to the SM particles in a way that leads to moderately strong washout, whereas $N_{2,3}$ couple much more strongly compared to typical realisations of the see-saw mechanism, such that large, purely flavoured asymmetries can be generated. Moreover, the imposed flavour symmetry implies that $M_2 \simeq M_3$, but it should be noted that as it is assumed that $M_1 \ll M_{2,3}$, only asymmetries from the decays of M_1 are considered and the scenario does not rely on a resonance effect. Since Leptogenesis takes place there during the decay of M_1 rather than during the oscillations of sterile neutrinos, it should be clear that the scenario from Ref. [17] is different from what is discussed in the present paper. This is also reflected by the difference in the viable parameter space in terms of the M_i that is found for both scenarios. (Here, the M_i may be substantially smaller.) Another variant of purely flavoured Leptogenesis with sterile neutrino masses above the electroweak scale is discussed in Ref. [18], where extra particles beyond the see-saw scenario are introduced.

The outline of this paper is as follows: In Section 2, we specify the way we calculate the BAU in the proposed model and in Section 3, we identify a viable point in parameter space and discuss some parametric dependencies. We conclude in Section 4.

2 Lepton Asymmetry and Washout

In this Section, we derive the equations that can be used to determine the freeze-out asymmetry in the ARS scenario with sterile neutrinos above the electroweak scale. While the initial flavoured asymmetries in the ℓ_a can be computed using the same techniques irrespective of whether the sterile neutrino masses are above or below the electroweak scale, the washout calculation must account for the fact that the sterile neutrinos become non-relativistic before the sphaleron transitions freeze out, in contrast to the original ARS proposal with sterile neutrinos below the electroweak scale. The most important consequence of this difference is that while the sterile neutrinos are relativistic, only flavoured asymmetries are washed out, whereas in the presence of non-relativistic sterile neutrinos, total lepton number is effectively violated by the Majorana masses as well.

Oscillations of the sterile neutrinos and CP violation.– We first consider the dynamics of the seesaw model when the sterile neutrinos are relativistic, *i.e.* $T \gg M_i$, and for a high reheat temperature of the SM particles. In particular, we discuss the generation of the initial lepton asymmetry that applies both, to the original ARS scenario and the situation with heavier sterile neutrinos above the electroweak scale, that is discussed for the first time in the present work.

While the Universe expands, the Higgs particle and leptons are maintained very close to thermal equilibrium through gauge interactions, while the sterile neutrinos may be far from equilibrium over a wide temperature range, because they are only interacting through the Yukawa couplings Y. As a plausible initial condition, we assume that the abundance of the sterile neutrinos vanishes. The sterile neutrinos are then produced from interactions with leptons and Higgs bosons. For $T \gg M_i$, the fastest processes involve the radiation of an extra gauge boson ($2 \leftrightarrow 2$ processes) [19, 20]. In contrast, for $T \ll M_{Ni}$, inverse decays ($2 \leftrightarrow 1$ processes) dominate.

Now, provided the matrix $YY^\dagger$ is non-diagonal, the sterile neutrinos emerge as superpositions of their mass eigenstates and oscillate. As a result, these coherently superimposed states can decay into leptons ℓ and Higgs-bosons ϕ in an asymmetric manner [13, 14]. This way of creating an asymmetry is often referred to as CP-violating from mixing. It is therefore interesting to note the temperature, at which the first oscillation is completed for a typical sterile neutrino with momentum of order of the temperature T. In order to quantify this, we define $a_{\rm R} = m_{\rm Pl}\sqrt{45/(4\pi^3 g_\star)}$, where $m_{\rm Pl}$ is the Planck mass and $g_\star$ the number of relativistic degrees of freedom of the SM at high temperatures. For the scale factor in the radiation-dominated Universe, we take $a(\eta) = a_{\rm R}\eta$, where η is the conformal time. By this choice, $T = 1/\eta$. Besides, we define $z = T_{\rm ref}/T = \eta T_{\rm ref}$. Note that the choice $T_{\rm ref} = M_1$ leads to the usual definition for the parameter z in Leptogenesis calculations [3]. In general, one may find it convenient to choose $T_{\rm ref}$ to be close to the temperature scale of interest, such that the parameter z is of order one during the relevant stages of the time-evolution. Within the final result for the freeze-out asymmetry, the arbitrary parameter $T_{\rm ref}$ drops out, of course. More than one full oscillation is

completed, when

$$\int_0^\eta \frac{|M_i^2 - M_j^2|}{2T} a(\eta) d\eta = \frac{\Delta M^2 a_{\rm R} \eta^3}{6} \gtrsim 2\pi \tag{2}$$

$$\Leftrightarrow \; z \gtrsim z_{\rm osc}^{ij} = \left[12\pi T_{\rm ref}^3/(a_{\rm R}|M_i^2 - M_j^2|)\right]^{\frac{1}{3}} \,,$$

what consequently defines $T_{\rm osc}^{ij} = T_{\rm ref}/z_{\rm osc}^{ij}$ and $T_{\rm osc} = T_{\rm osc}^{13}$, as the highest of these oscillation temperatures. Below $T_{\rm osc}^{ij}$, the oscillations can be averaged, what leads to a result in agreement with the usual perturbative calculations for the decay asymmetry of the sterile neutrinos [6, 7, 8, 9, 10, 11]. It can be shown that when averaging the oscillations, the time-dependence of the source term is $\propto 1/z^2$ [15]. Since washout becomes important at much later stages only, most of the asymmetry is produced around the temperature $T_{\rm osc}$. We recall at this point that for the conventional lepton-number violating contributions, the asymmetry is proportional to $M_i M_j/|M_i - M_j|^2$, while the purely flavoured source in the ARS scenario is enhanced by the factor $T^2/|M_i - M_j|^2$ [15]. The absence of the chirality-flipping insertions of Majorana mass thus explains why the ARS-type source yields much larger asymmetries at temperatures $T \gg M_i$ than the conventional source. The charge density $q_{\ell a}$ in the lepton flavour a that is dominantly produced at temperatures around $T = T_{\rm osc}$ is then given by [14, 15]

$$\frac{q_{\ell a}}{s} \approx - \frac{1}{g_w} \sum_{\substack{c \\ j \neq i}} {\rm i} \frac{Y_{ai}^\dagger Y_{ic} Y_{cj}^\dagger Y_{ja} - Y_{ai}^t Y_{ic}^* Y_{cj}^t Y_{ja}^*}{{\rm sign}(M_{ii}^2 - M_{jj}^2)} \tag{3}$$

$$\times \left(\frac{m_{\rm Pl}^2}{|M_{ii}^2 - M_{jj}^2|} \right)^{\frac{2}{3}} \times 8.4 \times 10^{-5} \gamma_{\rm av}^2 \,,$$

where s is the entropy density. Note that we take here a numerical factor that is slightly smaller compared to the one of Ref. [15], due to a more conservative estimate of $T_{\rm osc}$, see relations (2).

Note that Eq. (3) corresponds to a conservative estimate that may receive corrections of order one [15]. In particular, calculating the momentum-dependent phase-space distributions instead of solving for the number densities of the sterile neutrinos should improve the predictions. A complete leading order accurate calculation appears viable and will be tackled in the future. One can immediately verify that Eq. (3) implies that $\sum_a q_{\ell a} = 0$, because these asymmetries are purely flavoured. As stated in the introduction, it is important that at a later stage, the individual flavour asymmetries are affected differently by flavoured or LNV washout, such that eventually a total lepton asymmetry within the SM leptons arises. Note that differently from Ref. [15], we define q_X as the charge density within one component of the SU(2) multiplet, hence the factor $1/g_w$ with $g_w = 2$.

An important input parameter to Eq. (3) is $\gamma_{\rm av}$, the average production rate of sterile neutrinos. It is derived from the total production rate for N_i per unit volume, $[YY^\dagger]_{ii}\gamma^N$,

by dividing it with the number density of N_i:

$$\gamma_{\rm av} = \frac{\gamma^N}{2n_N^{\rm eq}}\,, \tag{4}$$

where $n_N^{\rm eq} = \int d^3k/(2\pi)^3\, f_{\rm F}^{\rm eq}(\mathbf{k})$ and $f_{\rm F}^{\rm eq}(\mathbf{k})$ is the Fermi-Dirac distribution of a massless fermion. It appears quadratic in Eq. (3), because one factor can be attributed to the available phase space and the other factor to the CP-violating cut. We take the value $\gamma^N = 2.2\times10^{-3}T^4$, where we have used $h_t = 0.6$, $g_2 = 0.6$ and $g_1 = 0.4$ for the top-quark Yukawa-coupling and for the SU(2) and U(1) gauge couplings, what should be suitable for an energy scale of $10^8\,$GeV. Consequently, $\gamma_{\rm av} = 0.012$, which is larger than the value used in Ref. [15]. The estimate there is based on a partial evaluation of the sterile neutrino production rate in the relativistic regime [19], while the complete leading-order results can be taken from the more recently published Refs. [20, 21]. Note that $\gamma^{\rm av}$ also appears in the flavoured washout rate in the relativistic regime, Eq. (8) below. Larger values for $\gamma_{\rm av}$ therefore enhance both the initial asymmetry and the washout, such that in view of the freeze-out asymmetry, theoretical uncertainties in this rate should be partly compensated.

One may take into account a temperature dependence due to the running coupling constants [19, 21], which we ignore here in view of the accuracy of other approximations used in the present calculation of the freeze-out asymmetry. In addition, we estimate the temperature $T_{\rm res}$, above which the largest of the widths of the sterile neutrinos exceeds the mass splitting, such that Eq. (3) should not be applied, as

$$T_{\rm res} = \sqrt{(M_2^2 - M_1^2)/(\gamma_{\rm av}\max_i[YY^\dagger]_{ii})}\,. \tag{5}$$

To summarise, the asymmetries $q_{\ell a}$ given by Eq. (3) are present after the initial oscillations of the sterile neutrinos at temperatures around $T_{\rm osc}$, but before sizable flavoured and LNV washout effects occur. We may therefore use the asymmetries (3) as initial conditions for Eqs. (14) or (A1) that describe the evolution of the flavoured asymmetries through washout. The time separation between the production of the initial asymmetries and their washout was first noted and made use of in a calculation in Ref. [14]. To explicitly validate this procedure within the present context, we define the temperature $T = T_{{\rm W}a}$ at which the rate for flavoured washout of ℓ_a equals the Hubble rate, $W_a^{\rm rel} = H$ [see Eq. (8) below], such that

$$T_{{\rm W}a} = m_{\rm Pl}\gamma_{\rm av}\sqrt{\frac{45}{4\pi^3 g_\star}}[Y^\dagger Y]_{aa}\,. \tag{6}$$

This should be compared with $T_{\rm osc}$, and in particular for the relevant flavour e, we must demand that $T_{{\rm W}e} \ll T_{\rm osc}$, for the separation of the initial production from washout to be valid. For our numerical example this comparison is made in Figure 3. We emphasise that expression (3) applies to both, the original ARS scenario with light sterile neutrinos as well as the scenario proposed here with sterile neutrinos above the electroweak scale,

and it can be obtained by integrating over the initial oscillations of the sterile neutrinos. It was first derived in Ref. [14], based on a density matrix description of the sterile neutrinos, following the original work [13]. Ref. [15] relies on an alternative method, using a Green-function description of the sterile neutrinos within a non-equilibrium framework. The analytic formula (3) does not only correspond to a simpler way of computing the asymmetry compared to numerically solving for the oscillations of the sterile neutrinos, it also transparently exhibits the dependence of the initial asymmetry on the model parameters[1].

Washout of left-handed leptons.– Below the temperature $T_{\rm osc}$, the asymmetry $q_{\ell e}/s$ given by Eq. (3) is approximately conserved initially until washout processes become important[2]. A net lepton asymmetry is then present at the time of sphaleron freeze-out during the EWPT, provided the individual lepton flavours are affected differently by the washout. For non-relativistic sterile neutrinos, the LNV washout rate of ℓ_a is usually obtained from the thermally averaged inverse decay rate, approximating the quantum statistical by classical Maxwell distributions [3]. In our parametrisation (in particular, using the dimensionless variable z as the time parameter), this quantity is given by

$$W_a^{\rm NR} = \sum_i Y^\dagger_{ai} Y_{ia} \left(\frac{M_i}{T_{\rm ref}}\right)^{\frac{5}{2}} \frac{a_{\rm R}}{T_{\rm ref}} \frac{3}{2^{\frac{7}{2}}\pi^{\frac{5}{2}}} {\rm e}^{-z\frac{M_i}{T_{\rm ref}}} z^{\frac{5}{2}} = \sum_i \bar{W}_i^{\rm NR} Y^\dagger_{ai} Y_{ia}\,, \tag{7}$$

while in the relativistic regime, the rate of equilibration of ℓ_a with the sterile neutrinos (*i.e.* the flavoured washout rate) is

$$W_a^{\rm rel} = \sum_i Y^\dagger_{ai} Y_{ia} \gamma_{\rm av} = \bar{W}^{\rm rel} \sum_i Y^\dagger_{ai} Y_{ia}\,. \tag{8}$$

One should note that the latter rate is lepton-number conserving, as it does not rely on the insertion of Majorana mass terms, which only enter at sub-leading order in the relativistic regime. Below, we consider a region in parameter space where $|Y_{ie}| \ll |Y_{i\mu}, Y_{i\tau}|$, such that only $q_{\ell e}$ is not nullified by washout, and any asymmetry that is transferred from $q_{\ell e}$ into relativistic sterile neutrinos will scatter or decay into $\ell_{\mu,\tau}$. We therefore take for the effective washout rate of ℓ_e

$$W_e = \sum_i Y^\dagger_{ei} Y_{ie} \big[\vartheta(T - M_i) \max(\bar{W}_i^{\rm NR}, \bar{W}^{\rm rel}) + \vartheta(M_i - T) \bar{W}_i^{\rm NR}\big]\,. \tag{9}$$

This accounts for the relativistic $2 \leftrightarrow 2$ scatterings at high temperatures (flavoured washout), for the $1 \leftrightarrow 2$ decays and inverse decays when $M_i \gtrsim T$ (LNV washout) and

[1] In particular, we remark that $q_{\ell a}/s$ can be of order 10^{-10} (*i.e.* of order of the observed BAU) even when the Yukawa interactions mediating between ℓ_a and the N_i are far from equilibrium, *i.e.* when $[Y^\dagger Y]_{aa} T_{\rm osc} \ll T_{\rm osc}^2/m_{\rm Pl}$ or equivalently $[Y^\dagger Y]_{aa} \ll (|M_{ii}^2 - M_{jj}^2|/m_{\rm Pl}^2)^{\frac{1}{3}}$.

[2] *Cf.* the evolution of the particular flavours shown in Figure 6 and the comparison between $T_{{\rm W}e}$ and $T_{\rm osc}$ in Figure 3. The temporal separation of the initial production of the asymmetry and the washout that mostly takes place at later stages is also made use of in Refs. [14, 15, 16].

eventually for the freeze-out of these reactions due to Maxwell suppression when $M_i \gg T$. Note that those Figures of Refs. [20, 21] that show the individual relativistic lepton-number conserving and the non-relativistic LNV contributions to the sterile neutrino production rate are well suited to illustrate the particular reactions we account for in the combined washout rate W_e, that is given by Eq. (9).

Complete and partial chemical equilibrium of right-handed SM leptons.– The Yukawa couplings h_a mediate chemical equilibration between the ℓ_a and R_a, at a rate that is given by $h_a^2 \gamma^{\mathrm{fl}} T$ with $\gamma^{\mathrm{fl}} = 5 \times 10^{-3}$ [22, 21]. Full equilibration implies $q_{\ell a} = q_{Ra} + \frac{1}{2} q_H$. (Note again our convention that the charge densities account for one component of a multiplet only. Hence, this relation follows from the condition for the chemical potentials $\mu_{\ell a} = \mu_{\mathrm{R}a} + \mu_H$, where $q_{\ell a,\mathrm{R}a} = \mu_{\ell a,\mathrm{R}a} T^2/6$ and $q_H = \mu_H T^2/3$.) Again, we ignore the temperature dependence of γ^{fl}, which is present because of running coupling strengths. The redistribution of the asymmetries is quantitatively relevant, because it reduces the washout rates, as only the ℓ_a couple to the sterile neutrinos. While chemical equilibrium between $\ell_{\mu,\tau}$ and $\mathrm{R}_{\mu,\tau}$ can be assumed for all temperatures below $1.3 \times 10^9\,\mathrm{GeV}$, we account for the possibility of only partial equilibration of ℓ_e and R_{e}. We include other spectator effects following Ref. [23]. In particular, we impose the following conditions:

(i) Chemical equilibrium is maintained by all SM Yukawa couplings but the electron-Yukawa coupling h_e. For the latter, we account for partial equilibration within the Boltzmann equations.

(ii) Strong and weak sphalerons are in chemical equilibrium.

(iii) The reactions mediating the process $\ell_{\mu,\tau} + \phi \leftrightarrow N_{1,2,3}$ are in equilibrium. (This of course must be verified for each particular choice of parameters made.) Note that in the relativistic regime, where $M_i \ll T$, these reactions involve at leading order the radiation of extra particles for kinematic reasons. We assign no chemical potentials to the N_i, as it is appropriate for the non-relativistic regime, where the Majorana masses M_i flip the sterile neutrino helicities. In the relativistic regime, one would need in principle a more refined description, tracking the number densities of the individual helicity states. As the washout of the initial asymmetry occurs mostly during the non-relativistic LNV regime, neglecting the finite rate of helicity flips should amount to a small correction only.

Regarding condition (i), we note that equilibrium of u- and d-quark Yukawa mediated interactions may not be an appropriate assumption within the higher range, above $2 \times 10^6\,\mathrm{GeV}$, for the sterile neutrino masses that we consider. Moreover, above $10^9\,\mathrm{GeV}$, s quarks and μ leptons should equilibrate as well. The low-mass region, that is perhaps the phenomenologically most interesting, should however not be affected by this simplification. For higher masses, the error incurred by not accurately treating the chemical equilibration of these non-leptonic interactions should be at the 10%–20% level [24].

In combination, above conditions force the relations

$$q_{\ell e} = -\frac{11}{26}\Delta_e - \frac{157}{390}q_{\mathrm{R}e}\,, \tag{10a}$$

$$q_H = -\frac{1}{13}\Delta_e + \frac{7}{195}q_{\mathrm{R}e}\,, \tag{10b}$$

where $\Delta_a = B/3 - 2q_{\ell a} - q_{\mathrm{R}_a}$ is the flavoured lepton asymmetry that is conserved by weak sphaleron processes, with B being the baryon charge density. (The factor 2 is due to our convention that $q_{\ell a}$ counts the charge within one component of the SU(2) doublet only.) In order to compute the final freeze-out asymmetry, we note that the total baryon-minus-lepton number density is

$$B - L = \Delta_e + \frac{8}{15}q_{\mathrm{R}e}\,. \tag{11}$$

Besides, it may be of interest to consider the effect of the partial chemical equilibration of the right-handed electron R_e by comparing the resulting asymmetry with the outcome in the two limiting cases of full chemical equilibrium and a vanishing chemical potential for R_e. For a vanishing chemical potential, we can set $q_{\mathrm{R}_e} = 0$ in above relations, whereas in the case of full equilibration, we obtain

$$q_{\ell\mathrm{e}} = -\frac{87}{277}\Delta_e\,, \qquad q_H = -\frac{24}{277}\Delta_e \tag{12}$$

and

$$B - L = \frac{237}{277}\Delta_e\,. \tag{13}$$

Final baryon asymmetry.– Putting together above details, equations that can be used to determine the BAU for the present scenario are simply given by (*cf.* Ref. [22]):

$$\frac{dq_{\Delta e}}{dz} = 2\,W_e\left(q_{\ell e} + \frac{1}{2}q_H\right)\,, \tag{14a}$$

$$\frac{dq_{\mathrm{R}e}}{dz} = -\,2\gamma^{\mathrm{fl}}\frac{a_{\mathrm{R}}}{T_{\mathrm{ref}}}h_e^2\left(q_{\mathrm{R}e} - q_{\ell e} + \frac{1}{2}q_H\right)\,. \tag{14b}$$

As initial conditions at $z = 0$, we take $q_{\mathrm{R}e} = 0$ and $q_{\ell e}$ obtained from Eq. (3). The solution evaluated at $z = T_{\mathrm{ref}}/T_{\mathrm{EW}}$ yields the e-lepton charge density $L_e = g_w q_{\ell e} + q_{\mathrm{R}e}$ at the EWPT. Due to the strong washout in the μ, τ flavours, there is no asymmetry in these sectors, and we obtain for the BAU $B \approx -(28/79)L_e$ [25], which is to be compared with the observed value $B_{\mathrm{obs}}/s = 8.6 \times 10^{-11}$ [26, 27].

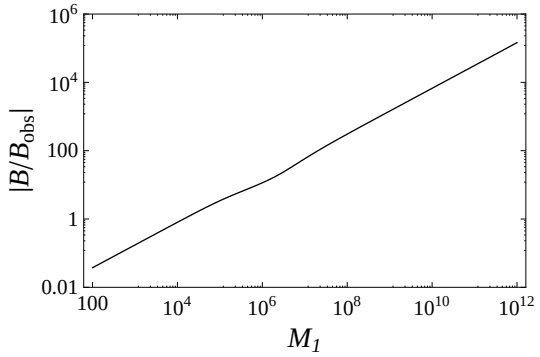

Figure 1: Final BAU normalised to the observed value for the reference parameters.

3 Example Scenario

Freeze-out asymmetry.– On the case of a specific parametric reference point, we demonstrate now that the proposed scenario can explain the BAU in a phenomenologically viable way. We use the parametrisation of the neutrino Yukawa couplings from Ref. [28] and follow the notation of Ref. [15]. For the mixing angles of the PMNS matrix and the mass differences of the SM neutrinos, we take the best fit values from Ref. [29]. We assume a normal mass hierarchy with the lightest neutrino mass $m_1 = 2.5\,\text{meV}$. As for the sterile neutrinos, we take $1:2:3$ for the mass ratios $M_1 : M_2 : M_3$. For the remaining angles, we choose

$$\begin{aligned} \delta =& 0.2\,, \quad & \omega_{23} =& 0.6 + 1.4\text{i}\,, \\ \alpha_1 =& 0\,, & \omega_{13} =& 0.1 - 1.5\text{i}\,, \\ \alpha_2 =& 2.6\,, & \omega_{12} =& -1.9 - 1.0\text{i}\,. \end{aligned} \tag{15}$$

We vary M_1, keeping the mass ratios of the sterile neutrinos fixed. In Figure 1, we show the ratio of the final BAU to the observed value as a function of M_1. It turns out that $B/B_{\rm obs} = 1$ for $M_1 \approx 4.8 \times 10^3\,\text{GeV}$ and $T_{\rm osc} \approx 2.2 \times 10^8\,\text{GeV}$. This value for $T_{\rm osc}$ can be interpreted as the minimum reheat temperature for the particular parametric scenario (15), and it happens to be somewhat below the corresponding value $2.0 \times 10^9\,\text{GeV}$ for standard Leptogenesis [3]. The increase of the asymmetry with M_1 can be easily understood in terms of the initial asymmetry (3) and the seesaw relation. The deviation from a simple power law, visible as a wiggle, is due to the equilibration of the spectator particles R_e, described by Eqs. (14). This feature is highlighted in Figure 2, where we compare the asymmetries from assuming either full or no chemical equilibration of R_e to the full result, solving for the asymmetry within R_e through Eqs. (14). The fact that the interpolation between the two limiting cases does not proceed monotonously is because initially larger asymmetries may be effectively hidden in the spectators before they fully equilibrate. This observation is related to the discussion of washout of primordial asymmetries of Ref. [22]. In the context of standard Leptogenesis, it is investigated in

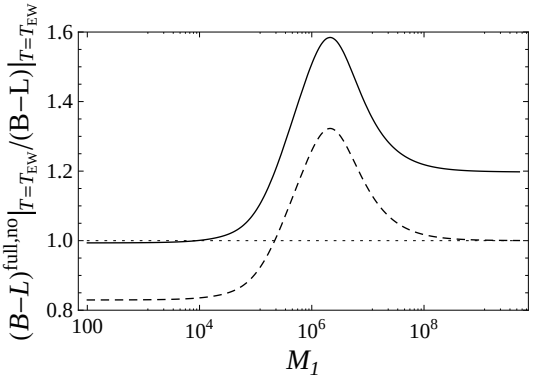

Figure 2: Ratio of the final BAU assuming either full equilibration (solid) or no equilibration of R_e compared to the result assuming partial equilibration for the reference parameters. The dotted line for the ratio one should help to guide the eye and to demonstrate that both limiting cases apply for small and large M_1.

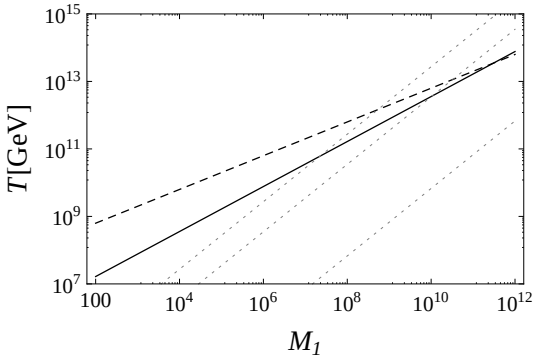

Figure 3: The temperature $T_{\rm osc}$ (solid) and the temperature $T_{\rm res}$ (dashed) for the reference parameters. The dotted lines represent $T_{{\rm W}e,\mu,\tau}$ from the bottom right to top left.

Ref. [30]. The mass range in which our approximations are viable is given by the condition $T_{\rm osc} < T_{\rm res}$, and from Figure 3, we see that we should choose M_1 to be below about 10^{11} GeV. We emphasise again that in the higher temperature range, the spectator fields such as the μ-lepton, and s, d, u quarks do not equilibrate, which we do not account of here, as we find the low mass range phenomenologically more interesting and the error of order 10% to 20% incurred [24] is comparable with other theoretical uncertainties in the present calculation. From Figure 3, we can also see that the approximation that we take in separating the production of the initial asymmetry in ℓ_e from its washout is met everywhere, since $T_{{\rm W},e} \ll T_{\rm osc}$.

Effective washout strength.– Within the studied range for M_1, we find that $(B-L)|_{T=T_{\rm EW}}/\Delta_e|_{T=T_{\rm osc}}$ varies between 0.2 and 0.17, *cf.* Figure 4, indicating that for the

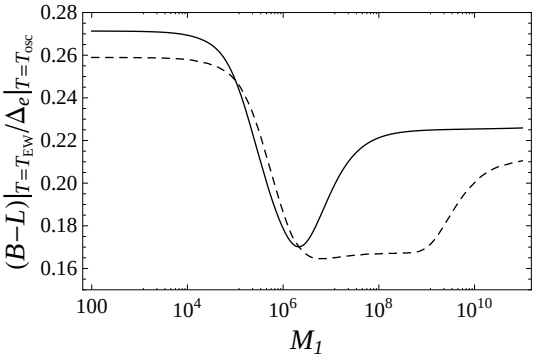

Figure 4: Fraction of the initial asymmetry that remains after washout for the reference parameters. Result based on the approximations described in Section 2 (solid), where the asymmetries in q_{Ni} and $\Delta_{\mu,\tau}$ are neglected are compared with the results from the equations of Appendix A (dashed), where the detailed evolution of the individual flavours are taken into account.

i \ a	e	μ	τ
1	0.25	2.0×10^2	1.8×10^3
2	0.46	2.3×10^2	1.9×10^3
3	0.35	1.7×10^2	1.1×10^3

Table 1: The washout parameters K_{ia} for the model specified through the reference point (15).

reference point, the $|Y_{ie}|$ takes small values such that the washout of the ℓ_e is as small as possible. We can verify this more explicitly in terms of the usual LNV washout parameters $K_{ia} = |Y_{ia}|^2 M_i/(8\pi H)|_{T=M_i}$. If $K_{ia} \gg 1$ for any of the N_i, the flavour ℓ_a suffers exponentially large washout, whereas for $K_{ia} \lesssim 1$, a substantial fraction of the asymmetry should survive. In Table 1 we list the explicit values for these washout parameters. From this, we see that indeed, sizeable asymmetries in the flavour e can persist down to the sphaleron freeze-out. Moreover, we see that quite the opposite is the case for the flavours μ and τ, what justifies our assumptions for calculating the asymmetry that are described in Section 2 [in particular assumption (iii)].

The moderately large imaginary parts of the mixing angles imply some tuning that may be estimated as $\cosh(\omega_{23})^2 \cosh(\omega_{13})^2 \cosh(\omega_{12})^2 \approx 60$, what implies that for our example, the Y_{ia} are generically about a factor eight larger than expected from the standard seesaw relation without a particular alignment. This amount of tuning can also be explicitly verified by observing cancellations of individual terms that add up to the largest of the light neutrino masses. Therefore, finding viable mixing angles for small M_i requires parametric tweaks. However, from Figure 1 it is clear that the situation becomes largely relaxed when allowing for larger M_i.

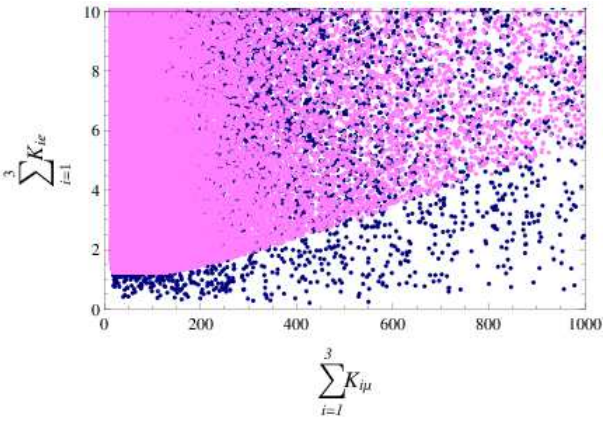

Figure 5: Washout parameters $\sum_i K_{ie,\mu}$ for a see-saw model with three sterile neutrinos in the mass ratio $1:2:3$ for $M_1 : M_2 : M_3$ and the light neutrino mass $m_1 = 2.5\,\text{meV}$, over a flat random distribution for the angles and phases δ, α_1, α_2, ω_{23}, ω_{13} and ω_{12} (dark blue). The same for a model with two sterile neutrinos (light magenta, implemented here by setting $m_1 = 0$, $\omega_{23} = 0$ and $\omega_{13} = \pi/2$).

Note that for our example point, we choose a scenario with three sterile neutrinos, whereas it is often useful to consider the limiting cases where one of these decouples or is simply not present. For such scenarios, it follows that one of the light neutrinos is massless, *i.e.* $m_1 = 0$ for normal neutrino mass hierarchy. However, the present scenario of Leptogenesis is most efficient, if the coupling of the flavour e to the sterile neutrinos is small, to suppress washout, while the couplings $Y_{i\mu}$ and $Y_{i\tau}$ should be large, what enhances the asymmetry (3). Of course, larger couplings Y_{ie} enhance the asymmetry as well, but this effect is substantially antagonised by the washout effect. The parameter scan presented in Figure 5 illustrates that favourable parametric configurations of the Yukawa couplings Y can better be achieved in a scenario with three sterile neutrinos when compared to the decoupling scenario, where an increase in the couplings $Y_{i\mu}$ automatically implies a larger lower bound on the couplings Y_{ie}.

Evolution of flavoured asymmetries prior to freeze out.– In the analysis presented to this end, we follow the evolution of the asymmetry within the flavour e but not within μ, τ because it should be subdominant at the time of freeze out. The reason is that for the parametric range that we investigate, the flavours μ, τ experience a much stronger washout than e. Besides, we neglect helicity asymmetries, that are present within the sterile neutrinos. At early times, when the Majorana masses are small compared to the temperature, lepton number L is approximately conserved when attributing the charge $L = 1$ to a positive-helicity sterile neutrino and $L = -1$ to a sterile neutrino with negative helicity. The approximate L-conservation during this regime of flavoured washout can be explicitly verified up to the point when the temperature becomes comparable to the mass of the sterile neutrinos and the LNV washout sets in.

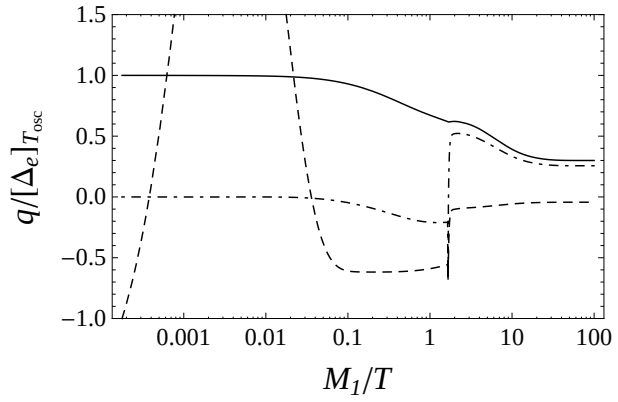

Figure 6: Evolution of various combinations of flavoured asymmetries for the reference parameters and with $M_1 = 2 \times 10^4\,\mathrm{GeV}$ after the initial oscillations at $z \approx z_{\rm osc}$: Δ_e (solid), $\Delta_\mu + \Delta_\tau$ (dashed), $\Delta_{\rm gen}$ (dot-dashed).

We therefore define the helicity-asymmetry density in the sterile neutrinos as

$$q_{Ni} = n_{Ni+} - n_{Ni-}\,, \tag{16}$$

where $n_{Ni\pm}$ are the number densities with helicity $\pm$, and we also introduce the generalised baryon-minus-lepton-number density

$$\Delta_{\rm gen} = \sum_{a=e,\mu,\tau} \Delta_a + \sum_i q_{Ni}\,. \tag{17}$$

Note that $\Delta_{\rm gen}$ is conserved in the limit $M_i \to 0$, what implies that it should remain close to zero for symmetric initial conditions before the temperature drops below the masses of the sterile neutrinos.

The evolution equations for the flavoured asymmetries are presented in Appendix A. In Figure 6, we present the evolution of particular asymmetries for the reference parameters, where we choose $M_1 = 10^5\,\mathrm{GeV}$. We can indeed verify that the asymmetry Δ_e is the only one that remains sizeable when $M_1/T \gg 1$. In turn the fact that the generalised baryon-minus-lepton asymmetry $\Delta_{\rm gen} \approx 0$ when $M_1/T \ll 1$ confirms the approximate conservation of the generalised lepton charge at early times. Note also that since $Y_{i\mu}$ and $Y_{i\tau}$ are much larger than Y_{ie}, the flavoured asymmetries asymmetries initially satisfy $|\Delta_{\mu,\tau}|_{T=T_{\rm osc}} \gg |\Delta_e|_{T=T_{\rm osc}}$, while lepton number conservation implies that $\Delta_\mu + \Delta_\tau|_{T=T_{\rm osc}} = -\Delta_e|_{T=T_{\rm osc}}$. The initial redistribution of the large asymmetries in the μ, τ sector to the sterile neutrinos therefore explains the strong initial incline of $\Delta_\mu + \Delta_\tau$. Note that it may also be instructive to compare Figure 6 with the schematic diagram explaining the various stages of ARS Leptogenesis presented in Ref. [16].

Note that Figure 6 also illustrates the main difference between the original ARS Leptogenesis scenario with sterile neutrinos below the electroweak scale to the present one with heavier neutrinos. While in the original setup, total lepton number is conserved

above the electroweak phase transition, implying that $\Delta_{\rm gen} = 0$ all the way down to $T_{\rm EW}$, we see that for the present scenario the LNV washout processes drive $\Delta_{\rm gen}$ to non-zero values around $T \approx M_i$[3]. As a result, there is a sizeable residual asymmetry $\sum_a \Delta_a = \Delta_{\rm gen} \neq 0$ within the active leptons at $T = T_{\rm EW}$, at which point no sterile neutrinos are present any more (such that $q_{Ni} \equiv 0$). This is in contrast to the original ARS scenario, where the active asymmetry is balanced by the helicity asymmetries in the sterile neutrinos, $\sum_a \Delta_a = -\sum_i q_{Ni}$, such that $\Delta_{\rm gen} = 0$.

In Figure 4, we also compare the results of the calculation of the freeze-out asymmetries based on the approximations of Section 2, where the initial evolution of the asymmetries in q_{Ni} and $\Delta_{\mu,\tau}$ is neglected, with the results from the equations of Appendix A. We observe that in the regimes of either full equilibration of R_e (small M_1) or no equilibration (large M_1), the calculation based on Section 2 underestimates the washout at the $5 - 10\%$ level. This can be attributed to the fact that opposite asymmetries stored in $\ell_{\mu,\tau}$ get transferred via helicity asymmetries in the N_i and then partly cancel the asymmetry in ℓ_e. The helicity asymmetries are accounted for in Appendix A but not in Section 2. Besides, the dip due to incomplete equilibration of R_e extends over a wider range when obtaining the results from Appendix A because the dynamics of the three different N_i are resolved individually.

4 Conclusions

We have studied the ARS mechanism for sterile neutrinos above the electroweak scale, what opens up a substantial region of parameter space for Leptogenesis based on the type-I seesaw model. While the generation of the initial flavoured lepton asymmetries proceeds in the same way as for the original ARS scenario with sterile neutrinos below the electroweak scale, the calculation of the washout must include LNV processes here, which is the main difference to the original proposal.

It is however possible to identify regions of parameter space where, while imposing the observed parameters from active neutrino mixing and oscillations, the initial asymmetry is large enough and yet the LNV washout small enough yield asymmetries that are of order of the observed BAU. In particular, we find that non-degenerate sterile neutrinos with masses substantially below $10^9\,\mathrm{GeV}$ may account for the BAU, what has not been found to be viable before and allows for new cosmologically consistent BSM scenarios. One should note however that the reheat temperature given by $T_{\rm osc}$ is by orders of magnitude above the mass scale of the sterile neutrinos [*cf.* Eq. (2)], unless assuming a mass degeneracy. Going to lower masses and reheat temperatures appears to require parametric tuning, either of the Yukawa couplings or the sterile neutrino masses, that should then be taken to be close to degenerate. (In turn, the source term that we discuss here generically adds asymmetries to scenarios of resonant Leptogenesis at low

[3]LNV processes are only important around these times, because for higher temperatures, sterile neutrinos are produced and destroyed mainly in lepton-number conserving scattering-processes, while at lower temperatures, the LNV decays and inverse decays of sterile neutrinos become Maxwell suppressed.

temperature scales.) Another option may be to extend the particle content of the model in such a way that the production of sterile neutrinos at the temperature $T_{\rm osc}$ becomes more efficient. It is interesting to note that the loop correction to the Higgs mass-square at the parameter point with the lowest viable sterile neutrino masses considered here ($M_1 = 4.8 \times 10^3\,\text{GeV}$) yields $\sum_i [YY^\dagger]_{ii} M_i^2/(16\pi^2) \approx (4 \times 10^{-2}\,\text{GeV})^2$, such that the electroweak scale is not necessarily destabilised by the sterile neutrinos, a desirable feature also emphasised in Ref. [31]. Future work on this scenario should encompass a more systematic analysis of the viable parameter space involving three sterile neutrinos as well as a more accurate determination of the relevant CP-violating rates.

Acknowledgements

This work is supported by the Gottfried Wilhelm Leibniz programme of the Deutsche Forschungsgemeinschaft (DFG) and by the DFG cluster of excellence Origin and Structure of the Universe.

A Including Helicity Asymmetries of the Sterile Neutrinos

In this Appendix, we extend the equations describing the washout of the e-flavour (14) to include as well μ, τ and the sterile neutrinos N_i. The resulting more detailed description of the washout is given by

$$\begin{aligned}
\frac{dq_{\Delta a}}{dz} =& 2\sum_i Y_{ia} Y_{ai}^\dagger \bar{W}_i^{\rm NR} \vartheta(M_i - T) \left(q_{\ell a} + \frac{1}{2} q_H \right) \qquad \text{(A1a)} \\
& + 2\sum_i Y_{ia} Y_{ai}^\dagger \max(\bar{W}_i^{\rm NR}, \bar{W}^{\rm rel}) \vartheta(T - M_i) \left(q_{\ell a} - q_{Ni} + \frac{1}{2} q_H \right) , \\
\frac{dq_{Ni}}{dz} =& 2\bar{W}^{\rm rel} \sum_a Y_{ia} Y_{ai}^\dagger \vartheta(T - M_i) \left(q_{\ell a} - q_{Ni} + \frac{1}{2} q_H \right) - 2\sum_a Y_{ia} Y_{ai}^\dagger \bar{\Gamma}_i^{\rm NR} \vartheta(M_i - T) q_{Ni} , \qquad \text{(A1b)} \\
\frac{dq_{{\rm R}e}}{dz} =& -2\gamma^{\rm fl} \frac{a_{\rm R}}{T_{\rm ref}} h_e^2 \left(q_{{\rm R}e} - q_{\ell e} + \frac{1}{2} q_H \right) , \qquad \text{(A1c)}
\end{aligned}$$

where $\bar{\Gamma}_i^{\rm NR} = a_{\rm R} z M_i/(16\pi T_{\rm ref}^2)$ is the decay rate of the sterile neutrinos [note the explicit factor of 2 in Eq. (A1b) that accounts for the SU(2)-multiplicity]. The helicity asymmetry in the sterile neutrinos q_{Ni} is defined in Eq. (16).

The relations between the asymmetries that appear on the left-hand sides of Eqs. (A1) to those on the right-hand sides are derived following the usual treatment of spectator

fields [23] and are given by

$$q_{\ell a} = \frac{1}{2886} \begin{pmatrix} -1221 & 156 & 156 & -1245 \\ 111 & -910 & 52 & 177 \\ 111 & 52 & -910 & 177 \end{pmatrix} \begin{pmatrix} \Delta_e \\ \Delta_\mu \\ \Delta_\tau \\ q_{\mathrm{R}e} \end{pmatrix} , \tag{A2a}$$

$$q_H = \frac{1}{481} \left(-37\Delta_e - 52\Delta_\mu - 52\Delta\tau + 45 q_{\mathrm{R}e}\right) . \tag{A2b}$$

In Eqs. (A1), flavoured and LNV washout rates are patched together at the point $M_i = T$. We can justify this by the fact that for smaller temperatures, the flavoured washout rates that are based on the production rates of relativistic neutrinos derived in Refs. [20, 21] should not be applicable, but are subdominant compared to the LNV rates, that rise steeply when T falls below M_i, *cf.* also the Figures that illustrate the sterile neutrino production rate as a function of temperature in Refs. [20, 21]. The steep incline of the relaxation rate of the sterile neutrinos once these become non-relativistic is also clearly reflected within Figure 6.

To increase the accuracy of the calculation, it would be desirable to use results for the production and relaxation of sterile neutrinos that are also valid between the relativistic and non-relativistic limits. Methods for calculating the production rate in this most general regime, where soft and collinear divergences lead to a substantial comlication of the situation, have been developed in Refs. [32, 33]. However, the numerical procedures are yet numerically challenging, such that a routine evaluation that could be used for the present purposes is not available yet. Moreover, neither of the Refs. [32, 33] distinguishes between LNV and lepton number conserving processes to this end. Including this is an important goal for extending these works in the future.

We also emphasise in this context, that the results for the sterile neutrino production are for simplicity typically reported for the total number density to date [20, 21, 32, 33]. Resolving the single momentum modes in the Boltzmann equations (*cf.* Ref. [34]) should improve the accuracy of calculations in ARS scenarios by order one, but these also increase the numerical efforts substantially.

References

[1] P. Minkowski, "$\mu \to e\gamma$ at a Rate of One Out of 1-Billion Muon Decays?," Phys. Lett. B **67**, 421 (1977); T. Yanagida, Progr. Theor. Phys. **64** (1980) 1103 ; M. Gell-Mann, P. Ramond and R. Slansky, in *Supergravity*, North Holland, Amsterdam 1980; R. N. Mohapatra and G. Senjanovic, "Neutrino mass and spontaneous parity nonconservation," Phys. Rev. Lett. **44** (1980) 912.

[2] M. Fukugita and T. Yanagida, "Baryogenesis Without Grand Unification," Phys. Lett. B **174** (1986) 45.

[3] W. Buchmüller, P. Di Bari and M. Plümacher, "Leptogenesis for pedestrians," Annals Phys. **315** (2005) 305 [hep-ph/0401240].

[4] S. Davidson and A. Ibarra, "A Lower bound on the right-handed neutrino mass from leptogenesis," Phys. Lett. B **535** (2002) 25 [hep-ph/0202239].

[5] S. Davidson, E. Nardi and Y. Nir, "Leptogenesis," Phys. Rept. **466** (2008) 105 [arXiv:0802.2962 [hep-ph]].

[6] L. Covi, E. Roulet and F. Vissani, "CP violating decays in leptogenesis scenarios," Phys. Lett. B **384** (1996) 169 [hep-ph/9605319].

[7] M. Flanz, E. A. Paschos, U. Sarkar and J. Weiss, "Baryogenesis through mixing of heavy Majorana neutrinos," Phys. Lett. B **389** (1996) 693 [hep-ph/9607310].

[8] A. Pilaftsis, "Resonant CP violation induced by particle mixing in transition amplitudes," Nucl. Phys. B **504** (1997) 61 [hep-ph/9702393].

[9] A. Pilaftsis, "CP violation and baryogenesis due to heavy Majorana neutrinos," Phys. Rev. D **56** (1997) 5431 [hep-ph/9707235].

[10] A. Pilaftsis and T. E. J. Underwood, "Resonant leptogenesis," Nucl. Phys. B **692** (2004) 303 [hep-ph/0309342].

[11] B. Garbrecht and M. Herranen, "Effective Theory of Resonant Leptogenesis in the Closed-Time-Path Approach," Nucl. Phys. B **861** (2012), 17. [arXiv:1112.5954 [hep-ph]].

[12] M. Garny, A. Kartavtsev and A. Hohenegger, "Leptogenesis from first principles in the resonant regime," Annals Phys. **328** (2013) 26 [arXiv:1112.6428 [hep-ph]].

[13] E. K. Akhmedov, V. A. Rubakov and A. Y. .Smirnov, "Baryogenesis via neutrino oscillations," Phys. Rev. Lett. **81** (1998) 1359 [hep-ph/9803255].

[14] T. Asaka and M. Shaposhnikov, "The nuMSM, dark matter and baryon asymmetry of the universe," Phys. Lett. B **620** (2005) 17 [hep-ph/0505013].

[15] M. Drewes and B. Garbrecht, "Leptogenesis from a GeV Seesaw without Mass Degeneracy," JHEP **1303** (2013) 096 [arXiv:1206.5537 [hep-ph]].

[16] B. Shuve and I. Yavin, "Baryogenesis through Neutrino Oscillations: A Unified Perspective," arXiv:1401.2459 [hep-ph]. This preprint appeared during the completion of the present manuscript and contains a comprehensive analysis of the parameter space in the model with two sterile neutrinos.

[17] S. Antusch, S. Blanchet, M. Blennow and E. Fernandez-Martinez, "Non-unitary Leptonic Mixing and Leptogenesis," JHEP **1001** (2010) 017 [arXiv:0910.5957 [hep-ph]].

[18] D. Aristizabal Sierra, L. A. Munoz and E. Nardi, "Purely Flavored Leptogenesis," Phys. Rev. D **80** (2009) 016007 [arXiv:0904.3043 [hep-ph]].

[19] A. Anisimov, D. Besak and D. Bodeker, "Thermal production of relativistic Majorana neutrinos: Strong enhancement by multiple soft scattering," JCAP **1103** (2011) 042 [arXiv:1012.3784 [hep-ph]].

[20] D. Besak and D. Bodeker, "Thermal production of ultrarelativistic right-handed neutrinos: Complete leading-order results," JCAP **1203** (2012) 029 [arXiv:1202.1288 [hep-ph]].

[21] B. Garbrecht, F. Glowna and P. Schwaller, "Scattering Rates For Leptogenesis: Damping of Lepton Flavour Coherence and Production of Singlet Neutrinos," Nucl. Phys. B **877** (2013) 1 [arXiv:1303.5498 [hep-ph]].

[22] J. M. Cline, K. Kainulainen and K. A. Olive, "Protecting the primordial baryon asymmetry from erasure by sphalerons," Phys. Rev. D **49** (1994) 6394 [hep-ph/9401208].

[23] R. Barbieri, P. Creminelli, A. Strumia and N. Tetradis, "Baryogenesis through leptogenesis," Nucl. Phys. B **575** (2000) 61 [hep-ph/9911315].

[24] E. Nardi, Y. Nir, J. Racker and E. Roulet, "On Higgs and sphaleron effects during the leptogenesis era," JHEP **0601** (2006) 068 [hep-ph/0512052].

[25] J. A. Harvey and M. S. Turner, "Cosmological baryon and lepton number in the presence of electroweak fermion number violation," Phys. Rev. D **42** (1990) 3344.

[26] G. Hinshaw *et al.* [WMAP Collaboration], "Nine-Year Wilkinson Microwave Anisotropy Probe (WMAP) Observations: Cosmological Parameter Results," Astrophys. J. Suppl. **208** (2013) 19 [arXiv:1212.5226 [astro-ph.CO]].

[27] P. A. R. Ade *et al.* [Planck Collaboration], "Planck 2013 results. XVI. Cosmological parameters," arXiv:1303.5076 [astro-ph.CO].

[28] J. A. Casas and A. Ibarra, "Oscillating neutrinos and muon to e, gamma," Nucl. Phys. B **618** (2001) 171 [hep-ph/0103065].

[29] G. L. Fogli, E. Lisi, A. Marrone, D. Montanino, A. Palazzo and A. M. Rotunno, "Global analysis of neutrino masses, mixings and phases: entering the era of leptonic CP violation searches," Phys. Rev. D **86** (2012) 013012 [arXiv:1205.5254 [hep-ph]].

[30] B. Garbrecht and P. Schwaller, "Spectator Effects during Leptogenesis in the Strong Washout Regime," arXiv:1404.2915 [hep-ph].

[31] V. V. Khoze and G. Ro, "Leptogenesis and Neutrino Oscillations in the Classically Conformal Standard Model with the Higgs Portal," JHEP **1310** (2013) 075 [arXiv:1307.3764].

[32] B. Garbrecht, F. Glowna and M. Herranen, "Right-Handed Neutrino Production at Finite Temperature: Radiative Corrections, Soft and Collinear Divergences," JHEP **1304** (2013) 099 [arXiv:1302.0743 [hep-ph]].

[33] M. Laine, "Thermal right-handed neutrino production rate in the relativistic regime," JHEP **1308** (2013) 138 [arXiv:1307.4909 [hep-ph]].

[34] T. Asaka, S. Eijima and H. Ishida, "Kinetic Equations for Baryogenesis via Sterile Neutrino Oscillation," JCAP **1202** (2012) 021 [arXiv:1112.5565 [hep-ph]].